Paper

A broadband multistate interferometer for impedance measurement

Piotr Szymański and Wojciech Wiatr

Abstract— We present a new four-state interferometer for measuring vectorial reflection coefficient from 50 to 1800 MHz. The interferometer is composed of a four-state phase shifter, a double-directional coupler and a spectrum analyzer with an in-built tracking generator. We describe a design of the interferometer and methods developed for its calibration and de-embedding the measurements. Experimental data verify good accuracy of the impedance measurement.

Keywords— impedance measurement, multistate interferometer, reflectometer.

1. Introduction

Vectorial reflection coefficient measurement may be performed today using various instruments. Besides the most popular vector network analyzers, there is a broad class of interferometers, in which the relationship between the incident and reflected waves on the tested device is established indirectly by measuring power of interfering different microwave signals that are linearly related to those waves. Within the class, there are instruments performing the measurement instantly (measurement multiports) or in successive steps (multistate reflectometers). The former group is represented by the well-known six-port junction [1], while the last one by multistate reflectometer [2] or AM/PM switched three port reflectometer [3]. All they yield almost the same number of measured powers necessary to unambigously determine the reflection coefficient.

As it has been shown in [3], sequential measurements made with one detector in several independent states of the switched three-port are equivalent to simultaneous readings from four detectors in the six-port junction. Since designers of the interferometers pursue for simplicity and lower cost, they tend to substitute the number of measurement states for the number of measurement ports at an expense of extended measurement time.

For automated measurement, the multistate interferometers use switched AM/PM modulators to realize different measurement states. Set of all amplitude and phase states realized by the modulator at a given frequency is typically depicted with points in polar coordinates and referred to as the modulator state distribution. Since accuracy of the impedance measurement depends on a particular state distribution, an optimal arrangement of the distributions in the whole frequency range is a challenging task for an instrument designer. As it was shown in [4], AM/PM switches of reflection type may operate over the bandwidth of few octaves, if properly designed.

The theory behind the reflection coefficient measurement using the six-port has been known for over quarter of a century [1] and can be applied to the multistate interferometers as well [2, 3]. There are two types of models that describe such a measurement, the linear and nonlinear ones and this results in the relevant calibration and accuracy enhancement techniques utilized for the multistate interferometers. Generally, the linear methods [5] are much simpler to implement in computer than the nonlinear ones [6], but usually utilize more unknown quantities and thus are more measurement extensive.

We present here a new four-state interferometer system for impedance measurement from 50 to 1800 MHz. The system employs a spectrum analyzer with an in-built tracking generator, a four-state phase shifter and a double directional coupler. The generator stimulates the measurement circuit through phase shifter and the coupler while the receiver of the spectrum analyzer measures the interfering waves in every phase-state of the shifter. We describe the shifter design and discuss two different models for the impedance measurement validating they usefulness with experimental measurements.

2. Multistate interferometer

A general scheme of the multistate interferometer is shown in Fig. 1a. The instrument measuring unknown impedance Z_x consists of a signal source, an AM/PM switch, a double directional coupler and a detector. In the kth state, the modulator produces two stimulating signals, a_{1k} and a_{2k}, that emerge then as the reflected waves b_{3k} and b_{4k} at relevant ports of the coupler. Due to mismatched terminations (the detector and Z_x), incident waves a_{3k} and a_{4k}, respectively, appear also at these ports. Consequently, all the waves interfere in the coupler's main line and the detector measures the resultant power. The measured power depends on the phase and magnitude relationships of both stimulating signals, which vary along with the modulator state. Generally, any stable receiver capable of measuring power may fulfil the detector's role.

The waves' interference can be explained using the equivalent circuit shown in Fig. 1b, where two wave sources b_{3k} and b_{4k} model the stimulation, and the reflection coefficient Γ_{rk} represents the receiver (detector) impedance for the kth state. The power measured by the receiver in this state is described by

$$P_k = \alpha_k \frac{|b_{3k} + \Gamma_x b_{4k}|^2}{|1 - \Gamma_x \Gamma_{rk}|^2} = c_k \frac{|\Gamma_x - q_k|^2}{|1 - \Gamma_x \Gamma_{rk}|^2}, \qquad (1)$$

where $q_k = -b_{3k}/b_{4k}$ is the reference point, i.e., the value of Γ_x for which the power drops to zero, and α_k and $c_k = \alpha_k |b_{4k}|^2$ are system constants. In the plane of the complex reflection coefficient Γ_x, formula (1) describes a family of cirles, being loci of constant power. The circles are excentric if the receiver is mismatched ($\Gamma_{rk} \neq 0$).

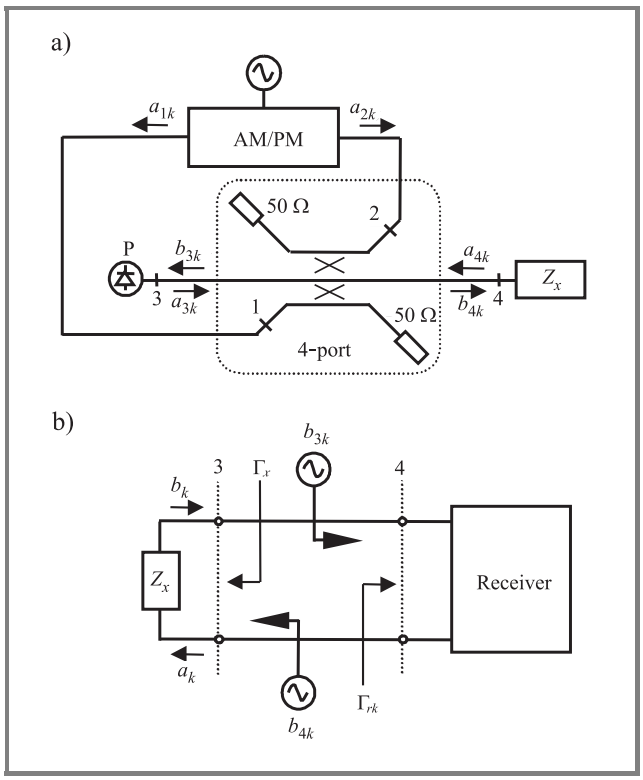

Fig. 1. Multistate interferometer: functional diagram (a) and its equivalent circuit (b).

There are five real parameters: c_k, $\mathrm{Re}\, q_k$, $\mathrm{Im}\, q_k$, $\mathrm{Re}\,\Gamma_{rk}$ and $\mathrm{Im}\,\Gamma_{rk}$, in formula (1). Therefore, calibration of the multistate interferometer requires, in general, measuring of at least five different impedance standards in each state to determine the unknown parameters. Considering K states of the interferometer, one gets the total of $5K$ calibration measurements. In case, when the input reflection coefficient of the receiver is invariant to the interferometer's state, the number of the unknowns reduces to $3K+2$ and thus fewer standards are necessary for the calibration.

3. Four-state phase shifter

We have decided to use a four-state phase shifter as our modulator and designed it considering availability and affordable costs of its components. The block diagram of the shifter is presented in Fig. 2. With the signal source

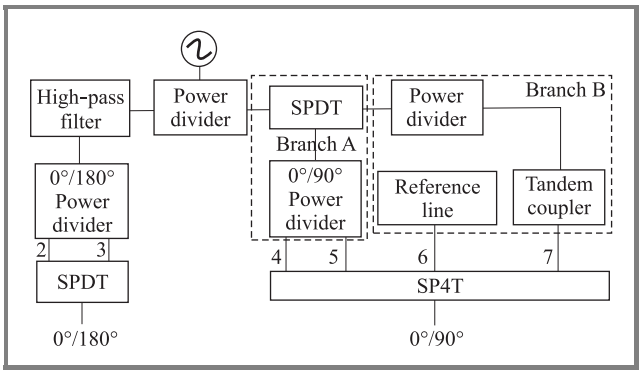

Fig. 2. Block diagram of the four-state phase shifter.

at the input, this three-port circuit produces two signals shifted in phase by 0° or 180° at one output and 0° or 90° at the other one. The phase shifts are realized by two specialized sections of this circuit, which are separated with the in-phase input power divider. Each section comprises a power divider whose outputs are shifted in phase and the phase keying rely on selecting the appropriate signal.

In contrast to the 0°/180° section, the 0°/90° section is composed of two branches, A and B, to provide coverage of the full frequency range. Due to limited bandwidth (50–700 MHz) of the 0°/90° commercial divider in branch A, the phase shifter in branch B, composed of another in-phase power divider, a tandem coupler and a reference line (a delay line), was built entirely in house for the upper subband (700–2000 MHz). The switches, single pole double throw (SPDT) and single pole four throw (SP4T) controlled by a microcontroller (not shown in Fig. 2), select the appropriate signals in each section, shifted in phase by: 0°, 90°, 180° or 270°. The phase shifts have been optimized in the whole frequency range using advanced design system (ADS), a microwave circuit simulator, on the basis of characteristics measured for the major components. To correct the phase at low frequency end, the high-pass filter (see Fig. 2) has been added in the 0°/180° section.

Distribution of the reference points can be evaluated from the three-port S parameters:

$$q_{ji} = \frac{S_{j1}}{S_{i1}}, \qquad (2)$$

where indices $i = 2,3$ and $j = 4,5,6,7$ regard relevant modulator's states in both subbands.

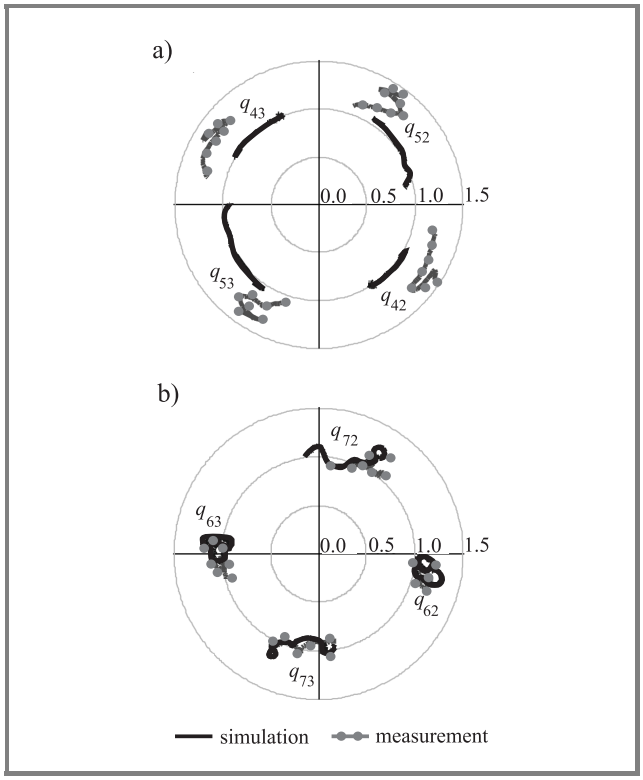

Fig. 3. Distribution of the modulator's phase states versus frequency in: lower (a) and upper (b) subbands.

Figure 3 shows frequency variations of (2) in the polar coordinates. The curves revolve similarly on each diagram thus maintaining almost 90° separation. The characteristics obtained by measurement and simulation in ADS are well matched, especially over the upper subband.

4. Calibration of multistate interferometer

Since in contrary to the six-port junction, the measurements made on the multistate interferometer do not comprise straight information on the incident wave in the circuit, the known six-port methods cannot be directly applied to calibration of the multistate interferometer. Therefore, we have developed our own method based on a linear model describing the measurements. For $\Gamma_{rk} = \Gamma_r = \text{const}$ ($k = 1, 2, 3, 4$) in formula (1), we write the equation:

$$\mathbf{x}\boldsymbol{\beta}_\mathbf{k} + p_k \mathbf{x}_\mathbf{p}\boldsymbol{\beta}_\mathbf{r} = p_k\,, \tag{3}$$

where p_k is a dimensionless power indication of the receiver in the kth state, the row vectors depend on Γ:

$$\mathbf{x} = \left[1-|\Gamma|^2 \quad 1+|\Gamma|^2 \quad -2\,\mathrm{Re}\,\Gamma \quad -2\,\mathrm{Im}\,\Gamma\right]$$

and

$$\mathbf{x_p} = \left[|\Gamma|^2 \quad 2\,\mathrm{Re}\,\Gamma \quad 2\,\mathrm{Im}\,\Gamma\right],$$

while the vectors $\boldsymbol{\beta}_\mathbf{k}$ and $\boldsymbol{\beta}_\mathbf{r}$ represent the system parameters:

$$\boldsymbol{\beta}_\mathbf{k}^\mathbf{T} = \frac{c_k}{2}\left[1-|q_k|^2 \quad 1+|q_k|^2 \quad -2\,\mathrm{Re}\,q_k \quad -2\,\mathrm{Im}\,q_k\right],$$

$$\boldsymbol{\beta}_\mathbf{k}^\mathbf{T} = -\left[|\Gamma_r|^2 \quad -\mathrm{Re}\,\Gamma_r \quad \mathrm{Im}\,\Gamma_r\right].$$

In the above formulae, the β parameters are nonlinearly related and this can be exploited to reduce the number of unknown coefficients in the Eq. (3) by $K+2$. The nonlinear relationships are as follows [7]:

$$\begin{aligned} \beta_{k2}^2 - \beta_{k1}^2 - \beta_{k3}^2 - \beta_{k4}^2 &= \boldsymbol{\beta}_\mathbf{k}^\mathbf{T}\mathbf{D}\boldsymbol{\beta}_\mathbf{k} = 0\,, \\ \beta_{r1}^2 - \beta_{r2}^2 - \beta_{r3}^2 &= \boldsymbol{\beta}_\mathbf{r}^\mathbf{T}\mathbf{D}_\mathbf{r}\boldsymbol{\beta}_\mathbf{r} - \mathbf{e}\boldsymbol{\beta}_\mathbf{r} = 0\,, \end{aligned} \tag{4}$$

where $\mathbf{D} = \text{diag}\ \{1\,{-}1\ 1\ 1\}$, $\mathbf{D_r} = \text{diag}\ \{0\ 1\ 1\}$ and $\mathbf{e} = [1\,0\,0]$.

For the system calibration, a set of known impedance standards $\{\Gamma_n\}$, $n = 1, 2, \ldots, N \geq 4$, is used and the measurements described by Eq. (3) can be set up in matrix form:

$$\mathbf{X_e}\boldsymbol{\beta} = \mathbf{y}\,, \tag{5}$$

where the vector $\boldsymbol{\beta}^\mathbf{T} = \left[\boldsymbol{\beta}_\mathbf{1}^\mathbf{T}\ \boldsymbol{\beta}_\mathbf{2}^\mathbf{T}\ \boldsymbol{\beta}_\mathbf{3}^\mathbf{T}\ \boldsymbol{\beta}_\mathbf{4}^\mathbf{T}\ \boldsymbol{\beta}_\mathbf{r}^\mathbf{T}\right]$ represents the unknown parameters, $\mathbf{y}^\mathbf{T} = \left[\mathbf{y}_\mathbf{1}^\mathbf{T}\ \mathbf{y}_\mathbf{2}^\mathbf{T}\ \mathbf{y}_\mathbf{3}^\mathbf{T}\ \mathbf{y}_\mathbf{4}^\mathbf{T}\right]$ comprises the measurements $\mathbf{y}_\mathbf{k}^\mathbf{T} = \left\{p_{kn}\right\}$ and the block coefficient matrix $\mathbf{X_e}$ is composed of matrices:

$$\mathbf{X} = \{\mathbf{x_n}\},\quad \mathbf{X_p} = \{\mathbf{x_{pn}}\}\ \text{ and }\ \mathbf{P_k} = \text{diag}(p_{kn})\,,$$

$$\mathbf{X_e} = \begin{bmatrix} \mathbf{X} & \mathbf{0} & \mathbf{0} & \mathbf{0} & \mathbf{P_1X_p} \\ \mathbf{0} & \mathbf{X} & \mathbf{0} & \mathbf{0} & \mathbf{P_2X_p} \\ \mathbf{0} & \mathbf{0} & \mathbf{X} & \mathbf{0} & \mathbf{P_3X_p} \\ \mathbf{0} & \mathbf{0} & \mathbf{0} & \mathbf{X} & \mathbf{P_4X_p} \end{bmatrix}.$$

The over-determined equation set (5) may be solved using a least squares method accounting for the constraints (4) [7]. For this purpose, we use the objective function:

$$\begin{aligned} L(\lambda, \beta) &= (\mathbf{y} - \mathbf{X_e}\boldsymbol{\beta})^\mathrm{T}\mathbf{W}(\mathbf{y} - \mathbf{X_e}\boldsymbol{\beta}) \\ &- \sum_k \lambda_k \boldsymbol{\beta}_\mathbf{k}^\mathbf{T}\mathbf{D}\boldsymbol{\beta}_\mathbf{k} - \lambda_r(\boldsymbol{\beta}_\mathbf{r}^\mathrm{T}\mathbf{D_r}\boldsymbol{\beta}_\mathbf{r} - \mathbf{e}\boldsymbol{\beta}_\mathbf{r})\,, \end{aligned} \tag{6}$$

where $\mathbf{W}$ is a diagonal weight matrix and the vector $\lambda = [\lambda_1\ \lambda_2\ \lambda_3\ \lambda_4\ \lambda_r]^\mathrm{T}$ comprises Lagrangian multipliers. We minimize (6) with a similar method as in [7] approaching the optimal solution iteratively. If the system is calibrated, reflection coefficients of measured devices are calculated in similar way as in [7].

5. Experimental results

For measurements, we arranged the interferometer in a measurement system shown in Fig. 4. The interferometer comprises the four-state shifter, a double directional

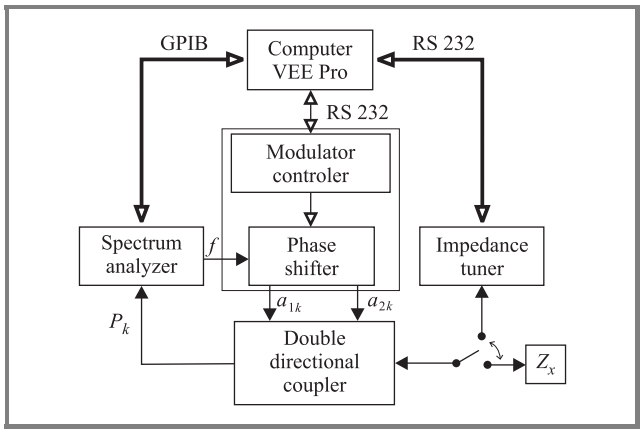

Fig. 4. Block diagram of the measurement system.

coupler and an HP8590L spectrum analyzer with in-built tracking generator. The generator stimulates the measurement circuit through phase shifter and the coupler while the spectrum analyzer measures the interfering waves at one port of the coupler's main line. The other port of this line is terminated with measured impedance Z_x. For the calibration, the system is equipped with an electronic impedance tuner that produces 36 known and repeatable values of the reflection coefficient [8]. All the system is controlled from a PC through GPIB and RS 232 communication buses using a program developed in VEE Pro environment [9].

The program enables user to perform the system calibration in two ways, with either a simplified or complete procedure. The simplified procedure assumes $\Gamma_{rk} = 0$ in the model (1) and in consequence $\boldsymbol{\beta}_\mathbf{r} = 0$ in (3)–(6). It may be, thus, applied to spectrum analyzers with well-matched input, e.g., using an attenuator. The simplified calculations go faster than in case of the complete procedure. This is achieved, however, at an expense of higher measurement uncertainty. Figure 5 shows this with two traces each for different procedure.

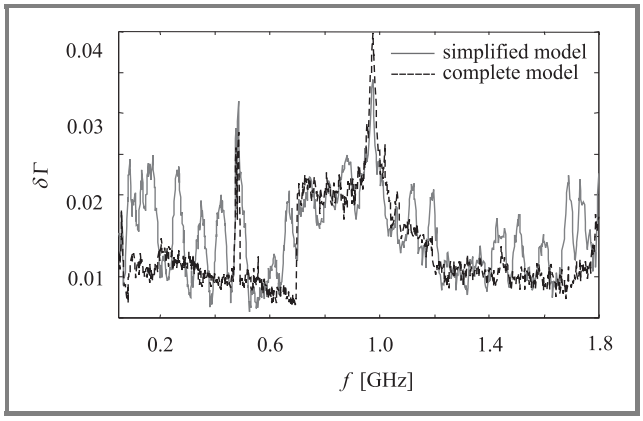

Fig. 5. Frequency dependence of the RMS error.

The graph in Fig. 5 illustrates frequency dependence of the root mean square (RMS) error of the reflection coefficient measurement in the system. The RMS error is calculated from deviations of the reflection coefficient:

$$|\Delta\Gamma| = |\Gamma_{MIF} - \Gamma_{VNA}|, \tag{7}$$

where Γ_{MIF} and Γ_{VNA} are the reflection coefficients measured using the multistate interferometer (MIF) and VNA, respectively.

The results shown in Fig. 5 refer all the reflection coefficients realized using the impedance tuner. The differences between both curves are not very pronounced due to the return loss of the receiver that was higher than 30 dB over the whole frequency range. Two prominent picks seen in the both curves are, perhaps, caused by interference coming from mobile communications bands. Thus except these two bands, the measurement uncertainty is less than 0.025.

6. Conclusions

We have presented a new multistate interferometer system for measuring vectorial reflection coefficient from 50 to 1800 MHz. The interferometer is composed of a four-state phase shifter that was designed in house, a double-directional coupler and a HP 8590L spectrum analyzer with an in-built tracking generator. The generator stimulates the measurement circuit through the shifter and the coupler while the spectrum analyzer measures the interfering waves in the coupler's main line. The reflection coefficient is determined from the measurements made for four phase states of the shifter. A PC controls the system and provides automation of the measurement process.

We described the design of the phase shifter, which was optimized in the whole frequency range to achieve the highest measurement accuracy as well as maintain low cost of the interferometer. The shifter's characteristics agreed well with the designed ones. We introduced also the technique we had developed for calibration of the system. The technique is based on a linear model and a LSQ method accounting for nonlinear constraints, which reduces the number of identified system parameters. We performed reflection coefficient measurements using the system and compared them with similar measurements made using a VNA. The experimental results have validated both the technique and high system's performance.

References

[1] G. F. Engen, "The six port reflectometer: an alternative network analyzer", *IEEE Trans. Microw. Theory Techn.*, vol. MTT-25, pp. 1075–1080, 1977.

[2] L. C. Oldfield and J. P. Ide, "A multistate reflectometer", *IEEE Trans. Instr. Meas.*, vol. 34, pp. 486–489, 1985.

[3] T. Morawski and M. Sypniewski, "AM/PM switched three port reflectometer", in *2nd Int. Symp. Meas. Electr. Quant.*, Warsaw, Poland, 1987, pp. 593–599.

[4] M. Szmidt-Szałowski and W. Wiatr, "A broadband design of a PM/AM switch for reflectometer system", in *Proc. 10th Microw. Conf. MIKON'94*, Książ, Poland, 1994, pp. 165–170.

[5] S. Li and R. G. Bossisio, "Calibration of multiport reflectometers by means of four open/short circuits", *IEEE Microw. Theory Techn.*, vol. 30, pp. 1085–1089, 1982.

[6] G. F. Engen, "Calibrating the six-port reflectometer by means of sliding terminations", *IEEE Trans. Microw. Theory Techn.*, vol. 26, pp. 951–957, 1978.

[7] W. Wiatr, "The multi-state radiometer: a novel means for impedance and noise temperature measurement", *IEEE Trans. Instr. Meas.*, vol. 46, pp. 486–489, 1997.

[8] D. Pieńkowski and W. Wiatr, "Broadband electronic impedance tuner", in *Proc. 14th Int. Microw. Conf. MIKON 2002*, Gdańsk, Poland, 2002, pp. 310–313.

[9] VEE Pro User' Guide. Agilent Techn. Inc., Santa Clara, CA, USA, 2000.

Piotr Szymański received the M.Sc. degree in electronic engineering from Warsaw University of Technology, Poland, in 2003. Since 2001, he has been with Telecommunications Research Institute (PIT), Poland. His current research include microwave circuits analysis and microwave measuerment system design. He is also interested in electronic support measures (ESM) systems and MMIC technology.
e-mail: szymanskip@pit.edu.pl
Telecommunications Research Institute
Poligonowa st 30
04-051 Warsaw, Poland

Wojciech Wiatr – for biography, see this issue, p. 22.